Bull Mar Sci. 96(4):735–752. 2020
https://doi.org/10.5343/bms.2020.0018

research tools in marine science

Subsurface automated samplers (SAS) for ocean acidification research

[1] *NOAA, Atlantic Oceanographic and Meteorological Laboratory, Ocean Chemistry and Ecosystem Division, 4301 Rickenbacker Cswy, Miami, Florida 33149*

[2] *University of Miami, Cooperative Institute for Marine and Atmospheric Studies, 4600 Rickenbacker Cswy, Miami, Florida 33149*

[3] *Gulliver Preparatory School, 6575 North Kendall Drive, Pinecrest, Florida 33156*

** Corresponding author email: <ian.enochs@noaa.gov>, telephone: 1-305-361-4399*

Ian C Enochs [1 *]
Nathan Formel [1, 2]
Lauren Shea [1, 2]
Leah Chomiak [1, 2]
Alan Piggot [3]
Amanda Kirkland [1, 2]
Derek Manzello [1]

ABSTRACT.—Ocean acidification (OA) is the process whereby anthropogenic carbon dioxide is absorbed into seawater, resulting in altered carbonate chemistry and a decline in pH. OA will negatively impact numerous marine organisms, altering the structure and function of entire ecosystems. The progression of OA, while faster than has occurred in recent geological history, has been subtle and detection may be complicated by high variability in shallow-water environments. Nevertheless, comprehensive monitoring and characterization is important given the scale and severity of the problem. Presently, technologies used to measure OA in the field are costly and limited by their detection of only one carbonate chemistry parameter, such as pH. Discrete water samples, by contrast, offer a means of measuring multiple components of the carbonate system, including parameters of particular explanatory value (e.g., total alkalinity, dissolved inorganic carbon), for which field-based sensors do not presently exist. Here we describe the design, use, and performance of a low-cost (<$220 USD) subsurface automated sampler (SAS), suitable for the collection of water for carbonate chemistry analysis. Each sampler is field-programmable using a remote control, performs in depths up to 55 m seawater, collects two separately preserved samples, and logs temperature at the time of collection. SAS are designed from the ground up to be open source with respect to physical design and sampling components, electronic hardware, and software. Build instructions, parts lists, and printable 3D files are provided along with code to ultimately lower the cost of OA monitoring, facilitate further research, and encourage application-specific customization.

Date Submitted: 29 March, 2020.
Date Accepted: 28 April, 2020.
Available Online: 29 April, 2020.

Ocean acidification (OA) is a global problem that, despite its apparently subtle progression, will have strong ramifications for ecosystems and economies worldwide (Hoegh-Guldberg et al. 2014). This is especially apparent in nearshore environments, where marine ecosystems are often in close proximity to coastal cities and provide services ranging from fisheries and tourism, to shelter from storm surge (Moberg and Folke 1999). In turn, overuse, pollution, and a lack of stewardship can place these ecosystems in a weakened state, where additional stressors can tip a tenuous balance toward collapse (Kennedy et al. 2013). Monitoring acidification and characterizing baseline carbonate chemistry is therefore of particular importance in these environments.

Nearshore processes also serve to increase variability, complicating characterization and making descriptions of coastal acidification especially challenging. Benthic and planktonic organisms can strongly influence carbonate chemistry, especially in shallow-water environments with restricted water exchange. Diurnal and seasonal cycles in productivity of these communities are accompanied by oscillations in the partial pressure of CO_2 (pCO_2) and pH (Price et al. 2012, Shaw and McNeil 2014). The same biological processes that drive these oscillations are significantly influenced by human activities and land-based sources of pollution, leading to periodic acidification hotspots (Duarte et al. 2013, Wallace et al. 2014, Enochs et al. 2019). Similarly, episodic events, such as storms, can lead to spikes in pCO_2 as respiration rises due to stress, and shading suppresses photosynthesis (Manzello et al. 2013). Despite this complexity, OA will only serve to enhance temporal variability and exacerbate the challenges of characterization (Shaw et al. 2012).

For these reasons, high-frequency measurements across large spatial scales is of paramount importance. Despite this urgency, climate-quality quantification of seawater carbonate chemistry remains problematic and costly. Two of the four carbonate system parameters [pH, pCO_2, total alkalinity (TA), dissolved inorganic carbon (DIC)] must be measured in concert with temperature, pressure, and salinity to solve the complete carbonate system. Instrumentation enabling direct high-frequency measurements in the field are on the market for two of these parameters (pH and pCO_2; Martz et al. 2015). With respect to pH, glass-bulb electrodes are fragile, prone to drift and biofouling, and are often supplied with calibration solutions which lead to the reporting of measurements on scales of limited utility to OA (NBS vs Total scale; Martz et al. 2015). Instruments that utilize solid state electrodes (ISFETs) or colorimetric determination of pH, while less prone to drift, can be costly and may require frequent calibration or refilling of reagents (Seidel et al. 2008, Martz et al. 2010). Instrumentation for the determination of pCO_2 in situ use either colorimetric methodologies or analysis of equilibrated gas (membrane or direct air/water equilibrator) using nondispersive infrared (NDIR) gas analyzers (Yoon et al. 2016). Prices range from >$10,000 to $100,000 USD and NDIR systems can be energy costly as well, due to the need for active water pumping and temperature regulation of the gas cell. The technology is consequently restricted to moored applications or benthic deployments tied to large battery packs (Jiang et al. 2014, Sutton et al. 2014).

Unlike instruments that record a single parameter, discrete seawater samples may be subsequently analyzed for all carbonate chemistry parameters in the laboratory. Provided that best practices are followed, samples can provide climate-quality data suitable for the characterization of OA and/or calibration of higher-frequency instrumentation (Dickson et al. 2007). Further, direct enumeration of DIC and TA can

provide insights into the biological processes controlling chemistry (Cyronak et al. 2018). One of the biggest limitations of this approach is that water samples generally require a collector onsite, as well as additional equipment (e.g., diving, Niskin rosette) if samples are to be taken at depth. Field time is costly and if samples are needed during challenging conditions when carbonate chemistry is often altered (e.g., storms, nighttime), collection may be impractical or unsafe.

Subsurface automatic sampling solutions suitable for carbonate chemistry are limited (Honda and Watanabe 2007, Albright et al. 2013). Commercially available devices are well tested and take numerous samples but are necessarily heavy, making them costly and potentially challenging to deploy (Honda and Watanabe 2007). The automated collection of water, however, is not inherently complicated, and several smaller solutions have been documented for a variety of applications (e.g., Martin et al. 2004, Higgins and Detweiler 2016). Several of these approaches are unsuitable for the collection of water for OA monitoring and there is an urgent need for small, simple, adaptable, and cost-effective technologies to address this sampling gap.

Recently, the "maker movement" has driven a rise in the accessibility of microcontrollers and hardware, along with open source software libraries (Cressey 2017). Advances in digital design, along with additive and subtractive manufacturing, have lowered barriers to development and fabrication. This has fostered an ethos of open-source science and instrument development, resulting in low-cost and rigorously-tested data loggers that can be built by nearly anyone (e.g., Beddows and Mallon 2018). Herein we apply this approach to water sampling, OA research, and monitoring by designing and testing an entirely open source subsurface automated sampler (SAS).

Materials and Methods

The SAS is a small (26 cm length), cost-effective (<$220 USD) submersible sampler that is capable of collecting two separate water samples of predetermined volume using peristaltic pumps and sampling bags (Fig. 1). The SAS is low-power and sampling times are field programmable using a remote control, without the need to expose water-sensitive electronics. There are two different modes of operation: (1) daily at a given time or (2) once for each of two pumps, at set times and dates. Temperature is recorded at the time of sampling on a microSD card.

The SAS can be built using tools and materials that are accessible and relatively low cost (Online Table S1). Detailed step-by-step instructions, component specifications and sources, design files (3D models and circuit board), as well as software necessary for construction are available at: https://www.coral.noaa.gov/accrete/sas/howtobuild.html. Online learning resources covering required skills are also on the site, along with links to companies that can 3D print, laser cut acrylic, and manufacture circuit boards, should a user/builder wish to outsource aspects of construction.

Physical Components.—The physical structure of the SAS was designed using the online CAD software Onshape (Onshape Inc.). The design utilizes a T-shaped housing of schedule 40 PVC, each of three ends of which are capped with a 3D printed flange (Fig. 1). The top face plate is laser cut from 0.25 in clear acrylic and mates to the flange with an O-ring seal. It is glued to a 3D-printed armature which holds the circuitry and battery pack. Access to the aforementioned is obtained via loosening bolts on the faceplate and sliding out the internal components. The lower two

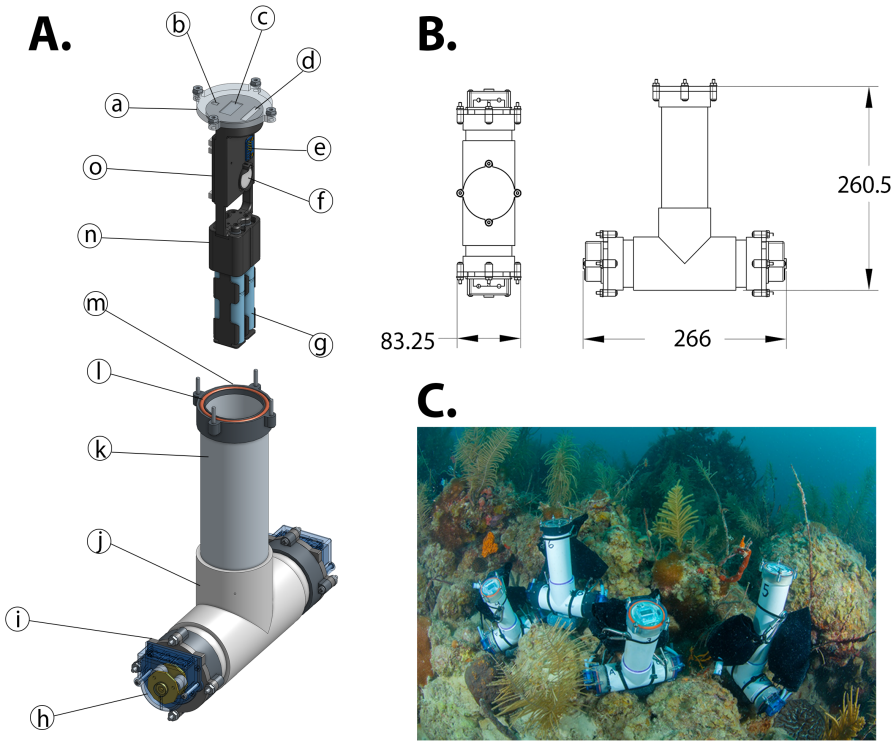

Figure 1. (A) Three dimensional CAD rendering of the SAS showing: (a) acrylic faceplate, (b) infrared detector, (c) OLED display, (d) magnetic switch, (e) temperature sensor, (f) coin cell battery for onboard clock, (g) AA battery packs, (h) peristaltic pump head, (i) waterproof motor faceplate, (j) PVC tee., (k) PVC pipe, (l) waterproof end cap flange, (m) O-ring, (n) internal armature, and (o) microcontroller and circuit board. (B) Dimensional (mm) drawing of external SAS housing. (C) Four SAS deployed at a coral reef as part of NOAA's National Coral Reef Monitoring Program (Photo credit K Davidson and ANGARI Foundation).

faceplates are also 3D printed and each have a DC gear motor seated to the faceplate using a printed bracket. The motor shafts extend through the faceplates and small X-rings seal the shaft-faceplate interfaces from water intrusion. OEM peristaltic pump heads (200-Series, Williamson Manufacturing Co. Ltd.) are affixed to the outside of the pump faceplate and a custom 3D-printed center adapter is used to mate the D-shaft of the gear motor to the pump head. All custom parts were printed and tested using a consumer-grade Form 2 stereolithography (SLA) 3D printer and standard Formlabs resins. Other SLA printers are likely suitable but remain untested.

When sampling, water is pumped through the selected peristaltic pump head and into sealed sample bags. Concentrated $HgCl_2$ solution is injected beforehand, through a septum on the sample bag in order to fix the sample and arrest biological processes which could subsequently alter carbonate chemistry. The Tedlar material has low CO_2 permeability but is relatively fragile, prone to puncture and tearing. Protective neoprene bags were laser cut to cover and protect the bags during deployment and collection (Fig. 1C).

Electronics.—Electronic hardware and circuitry were designed in Eagle (Autodesk, v8.5.2; Fig. 2). During the designing process, board prototypes were

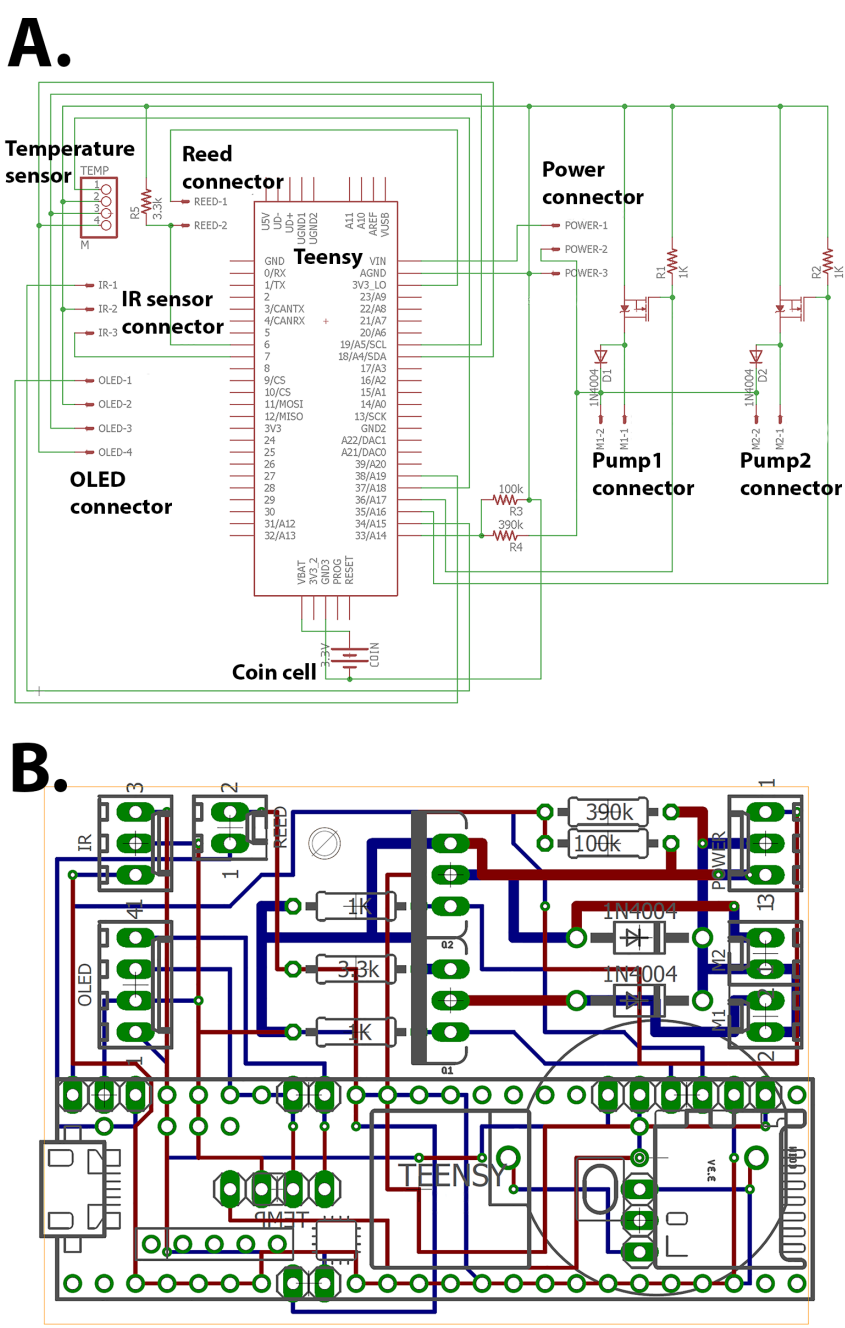

Figure 2. (A) Schematic showing connections between electronic components and connectors. (B) Circuit board layout: markings in green are pads and vias, red are paths on the top of the board, blue are on the bottom. Teensy Eagle footprint and symbol are by J Carruthers.

milled using two-sided copper plates and a desktop circuit board milling machine (Bantam Tools). Final circuit boards were produced by uploading Gerber files to Seeed Fusion (https://www.seeedstudio.io/fusion.html). Other printed circuit board (PCB) production companies will work but remain untested.

The Teensy 3.5 microcontroller (www.pjrc.com) was selected due to its low cost, low power capabilities, built in microSD card slot, and real-time clock (RTC). The Teensy 3.5 has a 32 bit 120 Mhz ARM Cortex-M4 processor, 512 kb of flash memory, 256 kb of RAM, 58 digital I/O pins, as well as I2C ports. The user interface is visible via a 0.96 in organic light-emitting diode (OLED) display, connected to the Teensy using the I2C communication protocol. Menu selection and sampling parameters are entered using an infrared (IR) remote control and a TSOP38238 IR receiver. A magnetic reed switch allows the user to wake up the SAS during low-power sleep mode and deployment. Temperature is determined at the time of sample collection using the MCP9808 I2C temperature breakout board (Adafruit). Motors are controlled using N-channel MOSFETs and battery voltage is measured on an analog input pin on the Teensy using a voltage divider.

Software.—The Teensy 3.5 is USB-programmable using the freely available Arduino IDE (www.arduino.cc), with the teensyduino add-on (www.pjrc.com). The SAS code relies on several freely available libraries (Online Table S2). The main program loop offers 10 cases, covering nine menu options and a sleep/operating state. Navigation between menus/states is done via IR remote control. Selecting "initiate" in the initiate menu begins the sleep process. The code checks if the pumps' sampling times are greater than 1 min in the future and, if so, calculates the number of seconds to the soonest programmed pumping event and puts the SAS to sleep for that amount of time. Wake-up is accomplished via an alarm at the programmed pumping time or a voltage on the reed switch interrupt pin. Upon wake-up, the SAS identifies which input has woken it. If it was the reed switch, it waits for half a second and confirms that the reed interrupt pin is high, two times. If the reed input is sustained, the SAS remains awake and defaults to the status menu. If not, the SAS assumes that it was an erroneous wakeup and it reinitiates the sleep/initiate process.

If the wake-up input is not the reed pin (i.e., the RTC alarm), the SAS checks alarm flags for each pump, executing the following logic for each independently. If the alarm flag is zero and the time is greater than the alarm time, the alarm is set to one. If the alarm flag is one, the corresponding pump is turned on, the time at which sampling should be finished is calculated, data is logged, and the alarm flag progresses to two. Sampling continues until the time is greater than the sample end time, at which point the alarm flag is set to three (finished) if the sampling mode is only a single collection time. If daily sampling is selected, however, the alarm flag is set back to zero and the alarm time is updated with an additional 86,400 sec (24 hrs). Upon updating the alarm flags and sample time, the SAS recognizes if the next alarm is within 1 min. If so, the process repeats; otherwise, the SAS returns to sleep mode.

Programming Collection Settings.—SAS are field programmable with an IR remote control. If the SAS is in a sleeping state, it should first be activated by placing a magnet next to the reed switch for more than 2 sec. The first initial menu gives the status of the SAS, including the time, temperature, deployment mode (once or daily), programmed collection time for each pump, volume to be collected, and

battery voltage. Pressing left or right buttons on the IR remote will advance the menu forward or backwards, respectively. The settings menu allows the user to select the sampling mode, as well as the volume of sample to be collected. In each menu where selections are made, the user must select and press enter over "ENTER SET" in order to save the settings to the SD card memory. The subsequent two menus allow the time of collection to be entered for pump A and B, respectively. If sampling mode is set to "daily," the date will refer to the date when the first daily collection will be made. The initiate menu allows the user to begin the sampling process. The time set menu is used to set the onboard real-time clock. The next menu (<PUMPCAL>) allows the user to enter calibration data for each pump, which is used to calculate the amount of time the pump will run in order to collect the desired water amount. The calibration numbers refer to the volume the specific pump samples in 10 sec, which can be determined using the next menu (<RUNCAL>). The final menu simply displays the software version and pressing right on the remote will cycle back to the first menu again.

IR remote programming works in day and nighttime conditions and has been demonstrated to work underwater, if the remote is sufficiently sealed in a waterproof bag. As an alternative to IR remote programming, all sampling parameters may be selected by directly modifying the SAMPLEPARAM.txt file on the SD card. The other file on the card (LOGDATA.txt) is where all sampling events are recorded, along with the temperature at time of sampling.

Field Deployment and Collection.—Following programming and initiation, SAS can be deployed underwater by diver, lowered over the side of a boat, left on the surface with extended sampling tubes, or however the user wishes to use them. SAS are positively buoyant but are generally stable (without additional securing) by attaching a 4 lb dive weight to their housing using a zip tie or hose clamp. Sampling bags should be labeled, secured inside neoprene protective sleeves prior to deployment, and connected to the outgoing tubes of the appropriate sampling pumps. Bags should be fixed prior to water collection by injecting concentrated $HgCl_2$ solution through the valve septum, without piercing the bag behind. Once connected to the pump tube, the valve should be opened one full turn to allow water to enter into the bag during collection. Bags should be removed and replaced prior to the subsequent sampling event if the sampler is placed in daily mode. The valve of filled sampling bags should be closed prior to removal from the pump head during retrieval and replacement. At the surface, bags should be inspected for punctures and placed in a safe place without sharp objects, such as a bucket of seawater. If analysis will not be conducted for a long period of time, it is recommended that the sample be transferred to a clean, rinsed borosilicate glass bottle with ground glass stopper, and sealed using carbon-free Apiezon grease and a rubber band, following guides for best practices (Dickson et al. 2007). Sample transfer from bag to bottle should be done in a manner to avoid gas exchange. A small length of tube from the bag to the bottom of the bottle will minimize turbulence and the introduction of air bubbles.

Assessment.—Several tests were conducted to evaluate the performance of the SAS. SAS were deployed numerous times in controlled laboratory aquaria to assess accuracy and precision, as well as by divers at sites ranging from healthy coral reefs, volcanic CO_2 vents, to navigational inlets in order to assess field performance and

usability. In one such laboratory experiment, multiple SAS were deployed in a tank at the University of Miami Experimental Reef Lab (ERL) and programmed to collect samples every 4 hrs for a period of roughly 3 d. The tank was programmed to have a diel pH oscillation of ±0.10 pH units around a mean of 8.00, using hourly dependent pH set points. Seawater pH treatments were accomplished via real-time measurements with a solid state pH electrode (Durafet, Honeywell) and computer regulated (custom LabVIEW software) addition of CO_2-free air and pure CO_2 was controlled with mass flow controllers (GFC, Aalborg, Enochs et al. 2018). The salinity of all collected samples was measured using a densitometer (DMA 5000M, Anton Paar). TA was determined using an AS-ALK2 (Apollo SciTech), which performs automated Gran titration. DIC was measured using an AS-C3 (Apollo SciTech). Duplicates were run for both TA and DIC. All values were corrected using certified reference materials following Dickson et al. (2007). Seawater pH (Total scale) was calculated using CO2SYS (Lewis and Wallace 1998) with the dissociation constants of Mehrbach et al. (1973) as refit by Dickson and Millero (1987) and Dickson (1990).

In order to assess the waterproof nature of the SAS housing, units were placed in water within a pressure chamber and repeatedly brought to 80 psi, equivalent to 55 m of seawater. The potential for pressure-constricted X-rings exerting additional friction on the motor shafts at depth and thereby reducing sample volumes was evaluated using a pressure chamber. Five SAS were programmed to collect 250 ml and then subjected to 0, 15, 44, and 73 psi (comparable to 0, 10, 30, 50 m seawater, respectively) in a random order. The accuracy and precision of the volume of water collected was evaluated by calibration of five separate SAS, which were each subsequently programmed to collect five different volumes of water (50, 200, 400, 600, 800 ml) in a random order. The resulting volumes of water collected were measured using a graduated cylinder and compared to the intended volumes.

In order to test the accuracy and precision of the onboard temperature loggers, two SAS were deployed in an indoor seawater system (ERL) where temperature was monitored using high-accuracy temperature probes (TTD25C, ProSense) and controlled (30.00 °C target ± 0.05 °C hysteresis) using custom LabVIEW software, a 300 W aquarium heater (TH-300, Finnex), and a solenoid-valve-operated titanium chiller coil (Hotspot Energy). Temperature was logged every 5 min by the high-accuracy control system, as well as each of the two SAS for a period of roughly 102 hrs, resulting in 1228 recorded measurements per instrument.

The current draw and battery longevity were tested two separate ways. First, five SAS were filled with eight fully charged NiMH AA batteries (1.2V, 2450 mAh, Eneloop pro, Panasonic) and the current draw was measured using a handheld multimeter (EX330, Extech Instruments) across the four-cell battery pack powering the control circuit, as well as the additional four-cells in series (eight total) used for pumping and voltage readings. Measurements were taken during sleep, in programming mode with the screen on, as well as during pumping. Power consumption over multiple sampling events was evaluated by programming (code was modified) one SAS with freshly charged batteries to sample 500 ml every 1 hr and the battery voltage was logged each time prior to sampling. All pumping was done under load, with water circulating through the pump.

The influence of several different factors on sample bag permeability and carbonate chemistry stability was evaluated with two separate experiments. In the first, to assess water sample stability, we examined the influences of temperature and time

since sampling on the carbonate chemistry of sealed (valve closed) Tedlar sample bags. Sample bags were rinsed prior to the experiment with approximately 100 ml of distilled water, which was immediately evacuated with a peristaltic pump. Following, 350 µL of a concentrated $HgCl_2$ solution was injected into each sample bag through the valve septum using a syringe. A 200 L batch of filtered (25 µm) seawater was poured into a tank and continuously mixed using pumps (Koralia Evolution 1500 GPH, Hydor) for a period of 3 hrs. Twelve samples (550 ml) were collected and immediately preserved in borosilicate glass bottles with 200 µL of a concentrated $HgCl_2$ solution. Five samples (750 ml) were pumped into the aforementioned rinsed Tedlar sample bags with preservative, and then immediately transferred into glass bottles. Thirty additional bags were prepared and filled in the same manner, and half were placed in a controlled water bath programmed to 22 °C, while the other half were maintained at a targeted 32 °C. Five bags were collected from each temperature treatment after 1, 7, and 14 d. All were subsequently transferred to borosilicate bottles and analyzed for TA and DIC. The remaining carbonate chemistry parameters (Ω_{arag}, pH, and pCO_2) were calculated using CO2SYS at 27 °C so that values could be directly compared across the two temperature treatments.

A second experiment was conducted to investigate the influence of bag type (Tedlar and Supel-Inert foil-lined bags, Supelco) and interbag pH gradient on the stability of preserved water samples. A homogenous batch of filtered seawater was created, and bags were rinsed and prepared with $HgCl_2$ preservative as in the prior experiment. Water samples (900 ml) were pumped into bags of each type (Tedlar and Foil). Five bags of each type were immediately transferred into borosilicate glass bottles, and another five of each type were submerged in each of three aquaria held at a different target pH (7.8, 7.9, and 8.0) using the system described in Enochs et al. (2018). Peristaltic pump heads were placed in-line with the valve inlets so that sealing was accomplished due to the pinching of the tube, as would occur during normal deployment. In order to minimize the potential for gas exchange through the pump tubing to alter sample chemistry, a one-way check valve (#80198, Qosina) was placed immediately after the bag valve before the pump tubing. Bag and pump head assemblies were kept in controlled seawater baths programmed to 22 °C for a period of 14 d. Following bag collection, samples were transferred to borosilicate glass jars, preserved, and analyzed for TA, DIC, and pH (spectrophotometric, following Carter et al. 2013). An irregularity in the performance of the DIC analyzer resulted in unreliable readings of that parameter. Accordingly, DIC, pCO_2, and Ω_{arag} were calculated using TA and pH with CO2SYS.

The salinity and carbonate chemistry of water samples preserved in borosilicate glass bottles were compared to those collected from Tedlar bags held at the 22 and 32 °C treatments for 14 d using one-way ANOVA, and Kruskal–Wallis tests when the data did not conform to the assumptions of a parametric test. The influence of ambient seawater pH on the carbonate chemistry and salinity of seawater samples contained in both bag types was examined using ANOVA and Kruskal–Wallis tests as above. Statistics were performed using RStudio (RStudio Team 2015), with the ggplot2 (Wickham 2009) used during initial data exploration.

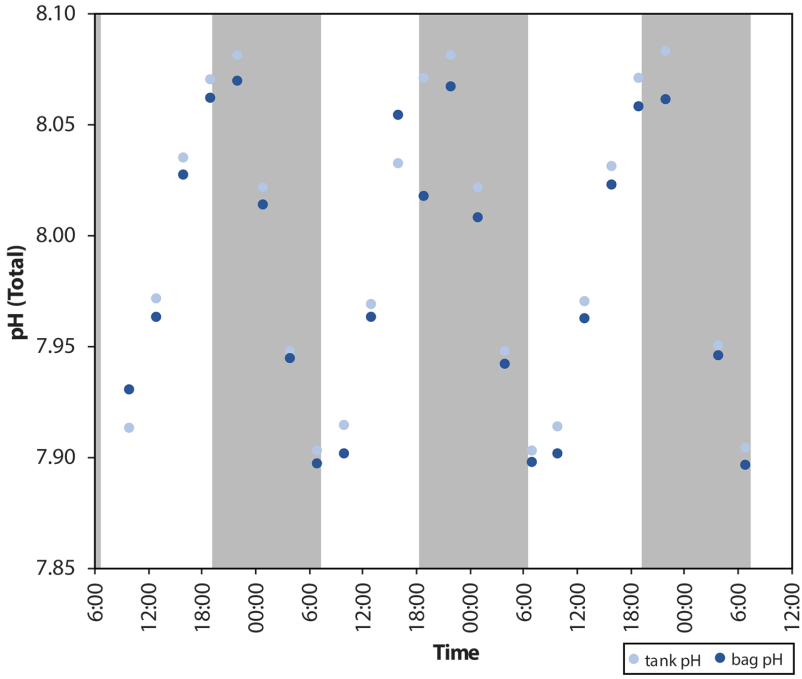

Figure 3. Variation in seawater pH as measured by Honeywell Durafet (light blue) and as calculated from DIC and TA, measured from water samples collected by SAS (dark blue). Tanks were programmed to have a pH oscillation of ±0.10 pH units around a mean of 8.00 and were controlled using automated gas injection (CO_2 and CO_2-free air) via Venturi valves and mass flow controllers.

Results

The 3D-printed SAS housings performed at depth with suitable strength and minimal flexion under pressures tested herein (55 m). No additional machining or processing was necessary to achieve these results. No water intrusion was observed around the motor shaft/X-ring seals during sampling (Fig. 1C) despite hundreds of collection events. SAS performed effectively in the field and lab, collecting water samples for analysis of carbonate chemistry. Calculated pH data (from water samples) were consistent [mean difference (SD) = −0.01 (0.01)] with dynamic pH oscillation treatments created in the lab and measured using a Durafet (Fig. 3).

Sample Volume.—There was no relationship between depth of deployment and the volume of sample collected over the pressure range tested (Fig. 4A). There was, however, a degree of variance in the exact volume of water collected, relative to the programmed value, and it qualitatively appeared to increase at greater volumes, requiring more sampling time (Fig. 4B). The mean deviation of the five SAS tested ranged from 0% (SD 0) to −12% (SD 1) over the depths tested. This error was highly dependent on the quality of the calibration (time vs volume sampled) of each SAS.

Power Consumption.—Current draw across the four-cell battery pack supporting the "brain" was 0.22 mA (SD 0.022) during sleep mode and 54.40 mA (SD 1.65)

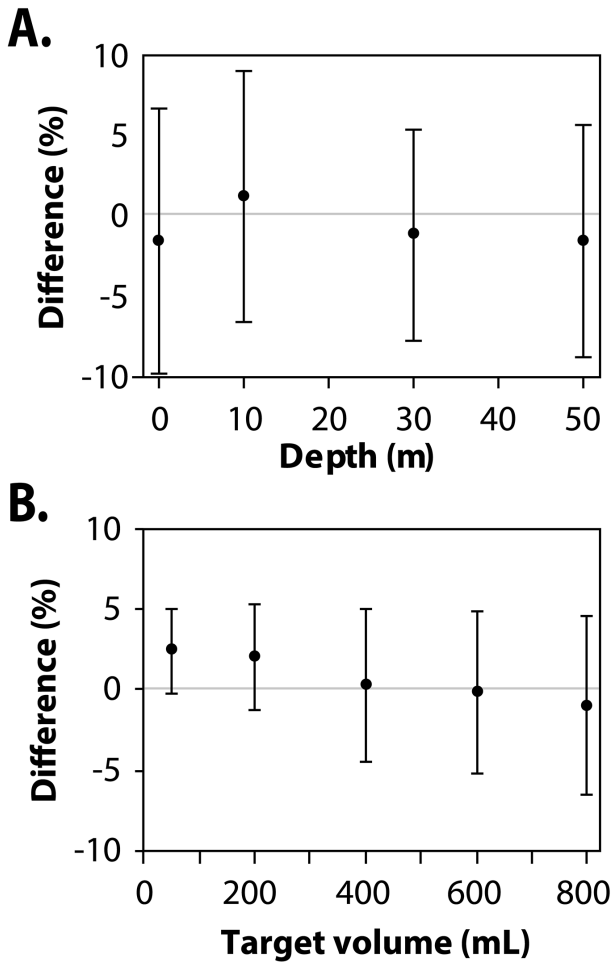

Figure 4. Percent difference in the volume of water programmed to be collected vs that collected as a function of (A) depth and (B) targeted volume. Error bars are standard deviations.

Table 1. Current consumption during three operational states: (1) running, while the pump is sampling water, (2) programming, while the OLED screen is on and receiving signals from an infrared remote control, and (3) sleep, while the SAS is dormant, waiting until the next sampling event. Current draw was measured across the four cells powering the microcontroller and electronic components (about 4.8V, brain), as well as all eight cells (about 9.6V, all) used to power the motors while pumping. Standard deviation in parentheses.

State	Battery pack	Current (mA)
Running	Brain	67.54 (0.57)
	All	373.04 (11.99)
Programming	Brain	54.40 (1.65)
	All	0.01 (0.00)
Sleep	Brain	0.22 (0.02)
	All	0.01 (0.00)

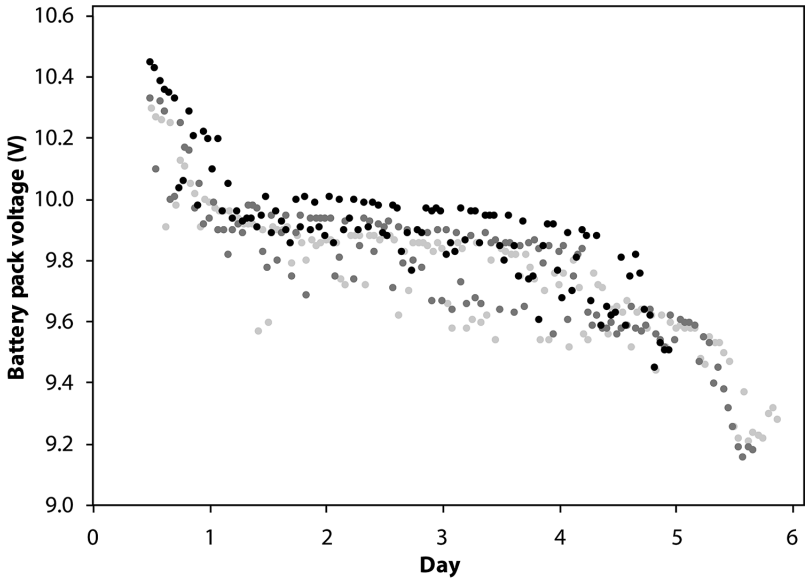

Figure 5. Change in battery pack voltage (eight AA NiMH cells, 2450 mAh, Eneloop Pro, Panasonic) of three SAS programmed to collect 500 ml of water every 1 hr. Battery voltage was recorded after each sampling event and logged internally on a micro SD card.

during programming (Table 1). Current consumption across the batteries used for motor power during these two modes was negligible (0.01 mA) and near the limits of detection of the instrument used. Considering a 2450 mAH battery pack and an arbitrary target of 25% of battery consumption, the logic battery pack should last for 116 d, or nearly 4 mo during deployment. The "brain" and "pump" battery packs consumed 67.54 mA (SD 0.57) and 373.04 mA (SD 11.99) during sampling (one pump), respectively (Table 1). Repeated hourly sampling of 500 ml for three separate SAS resulted in more than 4 d of sampling across the three units tested, comprising between 108 and 130 sampling events (about 54 and 65 L water, respectively) before voltage dropped too low for the instrument to continue (Fig. 5).

Temperature Measurement.—Temperatures recorded by SAS during evaluation were consistent with those recorded by high-accuracy temperature probes. During testing, recorded temperatures were 30.01 °C (SD 0.03), 29.87 °C (SD 0.10), and 29.81 °C (SD 0.08) for the high-accuracy temperature probe and two SAS, respectively. Equilibration from the internally housed temperature sensor, to that of the surrounding water bath was not instantaneous and, in the case of this test, took a period of time greater than 1 hr.

Parameter Stability.—The stability of salinity and carbonate chemistry parameters were examined for bags held in the 32 and 22 °C water bath treatments (Table 2). No significant differences were detected between the samples preserved in borosilicate glass bottles or in sealed Tedlar sample bags held in the two temperature treatments for 14 d (Table 2). Salinity was nonsignificant but near the alpha threshold (P = 0.05004). The range of all measurements considered in the test (control vs 14 d) was 0.14 and the difference between treatment means was 0.03.

Table 2. Salinity and carbonate chemistry of water samples preserved in Tedlar sampling bags held at 22 and 32 °C treatments for a period of 1, 7, or 14 d. Controls were collected in borosilicate glass bottles following best practices. Samples marked as immediate were collected in bags and immediately transferred to bottles. Carbonate chemistry data that were not directly measured are calculated at 27 °C to allow for cross-treatment comparison of drift. Test statistics given for ANOVA and Kruskal–Wallis (KW) tests used to analyze control bottles vs 22 and 32 °C-treated samples after 14 d in a one-way design. Standard deviations in parentheses. ns = not significant ($P \geq 0.05$). Sample size is five for each treatment with the exception of control bottles, of which 12 were taken.

	Temp (°C)	Salinity	DIC (μmol kg^{-1})	TA (μmol kg^{-1})	pH (Total)	pCO2 (μatm)	Ω_{arag}
Control bottles	- - -	33.48 (0.01)	2,169.1 (2.3)	2,434.4 (2.9)	7.96 (0.01)	548.1 (10.2)	3.21 (0.05)
Immediate	- - -	33.51 (0.02)	2,174.0 (1.1)	2,431.6 (1.8)	7.94 (0.00)	568.4 (6.0)	3.12 (0.03)
1 d	22	33.51 (0.01)	2,168.1 (2.2)	2,434.8 (4.2)	7.96 (0.01)	545.1 (8.3)	3.22 (0.04)
7 d	22	33.50 (0.01)	2,168.5 (1.6)	2,437.1 (1.6)	7.96 (0.00)	540.8 (5.0)	3.24 (0.02)
14 d	22	33.50 (0.01)	2,167.6 (2.0)	2,434.6 (5.1)	7.96 (0.01)	544.2 (12.0)	3.22 (0.06)
1 d	32	33.50 (0.00)	2,168.7 (1.3)	2,436.7 (1.8)	7.96 (0.01)	542.3 (7.3)	3.23 (0.03)
7 d	32	33.50 (0.01)	2,167.8 (1.3)	2,437.3 (1.0)	7.96 (0.00)	538.6 (4.9)	3.25 (0.02)
14 d	32	33.47 (0.06)	2,167.3 (2.5)	2,430.0 (2.6)	7.95 (0.00)	553.2 (5.2)	3.18 (0.02)
Control bottle vs 14 d at 22 and 32 °C	- - -	KW $\chi^2 = 5.99$, df = 2, ns	ANOVA $F_{(2,19)} = 1.47$, ns	ANOVA $F_{(2,19)} = 3.35$, ns	ANOVA $F_{(2,19)} = 1.15$, ns	ANOVA $F_{(2,19)} = 1.06$, ns	ANOVA $F_{(2,19)} = 1.25$, ns

Ambient seawater pH was not observed to have a significant effect on either the salinity or the carbonate chemistry of water samples held in foil or Tedlar bags (Table 3). Relatively high variability in the Tedlar 7.8 pH treatment was driven by two outlier pH readings, measured sequentially to be high and low, respectively.

Discussion

Design and Deployment Considerations.—

SAS successfully collected samples from a variety of field and lab conditions at different depths, temperatures, volumes, and deployment durations. Some field conditions, however, were observed to negatively impact instrument performance as tested. Long-term deployment in particularly high energy environments can lead to abrasion or tearing of thin Tedlar

Table 3. Salinity and carbonate chemistry of water samples collected in foil-lined and Tedlar sample bags. Samples were immediately transferred into borosilicate glass bottles (Control) or maintained in seawater held at targeted 8.0, 7.9, and 7.8 pH. Reported pH values are Total scale and were measured spectrophotometrically. All calculated values reflect the mean 22.15 °C conditions of the water baths. Test statistics given for ANOVA and Kruskal–Wallis (KW) tests used to analyze data in a one-way design. Standard deviation given in parentheses. ns = not significant ($P \geq 0.05$).

Bag type/ treatment	Temp (°C)	Salinity	TA (μmol kg^{-1})	pH (Total)	DIC (μmol kg^{-1})	pCO2 (μatm)	Ω_{arag}
Foil							
7.8	22.15	34.93 (0.15)	2447.0 (2.49)	7.979 (0.069)	2,187.4 (41.1)	496.9 (91.1)	3.01 (0.40)
7.9	22.15	34.98 (0.12)	2446.4 (2.08)	8.015 (0.007)	2,171.4 (5.1)	452.6 (9.5)	3.16 (0.04)
8.0	22.15	34.97 (0.12)	2446.8 (2.95)	8.015 (0.010)	2,173.7 (8.7)	457.1 (17.1)	3.14 (0.08)
Control	22.15	34.90 (0.06)	2445.7 (1.24)	8.009 (0.004)	2,177.8 (2.6)	467.2 (5.2)	3.09 (0.02)
	- - -	ANOVA $F_{(3,16)} = 0.636$, ns	ANOVA $F_{(3,16)} = 0.314$, ns	KW $\chi^2 = 4.844$, df = 3, ns	KW $\chi^2 = 5.183$, df = 3, ns	KW $\chi^2 = 6.017$, df = 3, ns	KW $\chi^2 = 6.035$, df = 3, ns
Tedlar							
7.8	22.15	35.05 (0.21)	2448.2 (1.30)	8.000 (0.026)	2,181.4 (14.8)	473.7 (33.9)	3.08 (0.15)
7.9	22.15	35.08 (0.06)	2449.5 (2.81)	8.013 (0.011)	2,177.8 (7.4)	462.4 (14.3)	3.12 (0.06)
8.0	22.15	35.01 (0.09)	2447.9 (2.77)	8.004 (0.015)	2,181.9 (3.5)	474.0 (9.5)	3.07 (0.04)
Control	22.15	34.95 (0.13)	2446.9 (1.79)	8.010 (0.004)	2,175.8 (1.7)	460.9 (4.6)	3.12 (0.03)
	- - -	ANOVA $F_{(3,16)} = 0.868$, ns	ANOVA $F_{(3,16)} = 1.074$, ns	KW $\chi^2 = 1.518$, df = 3 ns	ANOVA $F_{(3,16)} = 0.595$, ns	ANOVA $F_{(3,16)} = 0.677$ ns	ANOVA $F_{(3,16)} = 0.601$, ns

bags. While neoprene bag sleeves are helpful in ameliorating this in most situations, rigid PVC tubes (4 in diameter) were successful at protecting collection bags in especially high-flow channels, as well as shallow-water reef environments with strong wave action. Another deployment consideration is sedimentation. Especially turbid environments, as well as placement directly on sediments, can lead to, in some situations, blockage and obstruction of the sampling mechanism. This is particularly a concern for external moving parts, such as the roller carriage of the peristaltic pump. Care should be taken to make sure that these parts are protected from sand intrusion by placement on consolidated substrate or, when necessary, deployment on blocks or metal stakes immediately above the benthos.

The time it took for internal temperature sensors to equilibrate to the surrounding water bath during testing of the sensor's accuracy could be a concern in areas where temperature is changing drastically over minutes rather than hours, such as in upwelling areas or in stagnant, shallow-water pools. Sampling in areas with these types of dynamic temperature fluctuations should therefore be conducted in association with higher frequency temperature loggers that can more precisely record the temperature at the time of water collection.

While housing components, armatures, and faceplates printed with standard Formlabs SLA resins were watertight at depth and durable enough to withstand multiple lengthy field deployments, they were observed to be weaker than more traditional plastic materials. This was especially apparent for acute force where, for example, SAS housings that were dropped from about 1.5 m height cracked. In some situations, the 3D-printed roller carriage of the external peristaltic pump heads were observed to wear down around the motor shaft. This was observed to usually accompany other issues, such as a blocked pump. While not tested herein, the peristaltic pump head manufacturer (Williamson) now makes a carriage that accepts the motor shaft diameter. Printing of this part may therefore no longer be needed, thereby eliminating this concern. To increase strength and durability, parts can be machined or molded from other materials using the provided CAD files. Thermoplastic injection molded end caps and motor mounts were tested and found to be more durable than 3D prints. Tooling has been created at Protomold.com and Xometry.com, and the motor mount is publicly available upon request from Protomolds. While parts are cheaper per item, an initial setup fee is generally required.

Water Chemistry Stability.—Evaluation of the carbonate chemistry stability supports the viability of sampling bags for carbonate chemistry collection. Neither bag type nor temperature had a detectable influence on the carbonate chemistry of samples maintained for 14 d in ambient seawater (Table 2) and no drift was detected in an additional 14-d experiment, despite a strong pH gradient across the bag material (Table 3). Various tubing materials (e.g., Viton, PVC, silicone) may exhibit CO_2 permeabilities greater than Tedlar or foil sampling bags. Care should be taken to use low-permeability tubing or shorter lengths of tube with less surface area. Additionally, gas exchange across these materials can be reduced by restricting movement of the sampled seawater back into the tube, as was accomplished during evaluation with one-way check valves. Further testing should be conducted before sampling in more extreme conditions or if samples are to be left in bags for greater durations than those evaluated herein.

While differences were not significant ($P = 0.05004$) and the overall range was low, variability in salinity could have been introduced during bag processing, especially during rinsing. Moisture in the bag could lower salinity as observed in bag vs control bottles in Table 1. Conversely, salt residue from prior samples could have the opposite effect. During initial and repeat use, care should be taken to rinse and thoroughly dry sample bags to avoid these types of errors. Additionally, it is noted that larger sample volumes are proportionally influenced less by bag-related sources of error, including salts or trapped air bubbles. Programming SAS to collect more water may therefore provide more accurate data.

Where possible, paired instrumentation and water sampling are more powerful for assessing and ensuring data quality. Ultimately, borosilicate glass bottles are more solid and likely result in greater sample stability than bags. When possible, the amount of time water is maintained in a bag should be minimized, and samples should be carefully transferred to bottles and sealed following best practices for long-term storage. Using this approach, SAS were capable of accurately capturing high-magnitude diurnal oscillations of 0.20 pH units (Fig. 3) as well as during multiple field deployments (e.g., Enochs et al. 2020).

Future Directions.—The open source design of the SAS lends itself to modification. Numerous build-plans for water-tight housings are available (Beddows and Mallon 2018) and low-cost customizable options can be purchased commercially (e.g., bluerobotics.com). If the availability of 3D printing equipment is a limitation, it should be possible to suspend the battery packs and circuitry within a housing, thereby eliminating the need for an internal armature. Similarly, hand-cutting and drilling flanges, faceplates, motor brackets, and pass-throughs should all be feasible, though have not been tested herein. Modification to the low-power and watertight core components of the SAS should also be possible to allow for additional applications, including the addition of sensors and alterations to sampling frequency or triggering. Pumps or multi-position valves could be added to increase the number of collected samples, though the addition of these features may significantly alter cost and size. Finally, collection of samples for other water quality measurements is feasible (suspended sediments, nutrients, eDNA, etc.), though preservation and sample stability should be rigorously tested, and best practices developed beforehand.

The recent proliferation of accessible sensors and microcontrollers will help facilitate the democratization of OA research, and potentially other avenues of scientific inquiry with high associated costs (Cressey 2017). It is important, however, that this increase in accessibility proceeds in lockstep with evaluation, including careful quantification of performance and data quality (Riebesell et al. 2011). Significant financial barriers remain with respect to the determination of carbonate chemistry parameters. While the SAS reduces the cost of sample collection and simplifies complicated field logistics, it is still necessary to analyze the collected water samples. Analytical equipment can be costly or prone to error, and the certified reference material necessary for proper calibration can be expensive as well. Presently, the most accessible carbonate system parameters which can be accurately quantified from discrete water samples include pH and TA. By far, the most precise technique for pH determination is spectrophotometric, though instrumentation is expensive. Advancements are being made with respect to solid state pH electrodes, though high-quality glass bulbs calibrated with Tris buffers can be used at a lower price point, as long as temperature

is accurately quantified/controlled. Autotitrators for TA determination (gran titration) exist for >$2000 USD, though principles and components of measurement, automation, and control are accessible and relatively cheap, potentially presenting a viable means for the next step in open-source OA research. To date, high quality instrumentation for the assessment of DIC remains expensive (>$10,000 USD) and pCO_2 analysis of discrete water samples is problematic due to the large volumes needed for air/water equilibration.

By reducing the logistical requirements and financial costs for sample collection, SAS will facilitate greater characterization of carbonate chemistry variation across temporal and spatial scales. This information is critical for documenting the progression of global OA and for describing the complex carbonate chemistry of nearshore ecosystems. As research continues to reveal the importance of variability in modulating biological responses to OA, these data will lead to more comprehensive modeling and better predictions of ecosystem responses.

Acknowledgments

Funding for SAS development was provided by NOAA via an Ocean Technology Development grant. Instrumentation for analysis of carbonate chemistry was funded through NOAA's Ocean Acidification Program and equipment for experimentally manipulating carbonate chemistry was funded through NOAA Ocean and Atmospheric Research's Omics Initiative. We are grateful for the assistance of A Boyd during analysis of carbonate chemistry, G Almela and M Jankulak during the construction of the instructional website, and M Gay during the design process.

Literature Cited

Albright R, Langdon C, Anthony KRN. 2013. Dynamics of seawater carbonate chemistry, production, and calcification of a coral reef flat, central Great Barrier Reef. Biogeosciences. 10:6747–6758. https://doi.org/10.5194/bg-10-6747-2013

Beddows PA, Mallon EK. 2018. Cave Pearl data logger: a flexible Arduino-based logging platform for long-term monitoring in harsh environments. Sensors (Basel). 18(2):530. https://doi.org/10.3390/s18020530

Carter BR, Radich JA, Doyle HL, Dickson AG. 2013. An automated spectrometric system for discrete and underway seawater pH measurements. Limnol Oceanogr Methods. 11(1):16–27. https://doi.org/10.4319/lom.2013.11.16

Cressey D. 2017. Age of the Arduino. Nature. 544:125–126. https://doi.org/10.1038/544125a

Cyronak T, Andersson AJ, Langdon C, Albright R, Bates NR, Caldeira K, Carlton R, Corredor JE, Dunbar RB, Enochs I, et al. 2018. Taking the metabolic pulse of the world's coral reefs. PLOS ONE. 13(1):e0190872. https://doi.org/10.1371/journal.pone.0190872

Dickson AG. 1990. Thermodynamics of the dissociation of boric acid in synthetic seawater from 273.15 to 318.15 K. Deep-Sea Res. 37(5):755–766. https://doi.org/10.1016/0198-0149(90)90004-F

Dickson AG, Millero FJ. 1987. A comparison of the equilibrium constants for the dissociation of carbonic acid in seawater media. Deep-Sea Res. 34(10):1733–1743. https://doi.org/10.1016/0198-0149(87)90021-5

Dickson AG, Sabine CL, Christian JR. 2007. Guide to best practices for ocean CO_2 measurements. PICES Special Publ. 3. 191 p.

Duarte CM, Hendriks IE, Moore TS, Olsen YS, Steckbauer A, Ramajo L, Carstensen J, Trotter JA, McCulloch M. 2013. Is ocean acidification an open-ocean syndrome? Understanding

anthropogenic impacts on seawater pH. Estuaries Coasts. 36:221–236. https://doi.org/10.1007/s12237-013-9594-3

Enochs IC, Formel N, Manzello D, Morris J, Mayfield AB, Boyd A, Kolodziej G, Adams G, Hendee J. 2020. Coral persistence despite extreme periodic pH fluctuations at a volcanically acidified Caribbean reef. Coral Reefs. https://doi.org/10.1007/s00338-020-01927-5

Enochs IC, Manzello DP, Jones PR, Aguilar C, Cohen K, Valentino L, Schopmeyer S, Kolodziej G, Jankulak M, Lirman D. 2018. The influence of diel carbonate chemistry fluctuations on the calcification rate of *Acropora cervicornis* under present day and future acidification conditions. J Exp Mar Biol Ecol. 506:135–143. https://doi.org/10.1016/j.jembe.2018.06.007

Enochs IC, Manzello DP, Jones PR, Stamates SJ, Carsey TP. 2019. Seasonal carbonate chemistry dynamics on Southeast Florida coral reefs: localized acidification hotspots from navigational inlets. Front Mar Sci. 6:160. https://doi.org/10.3389/fmars.2019.00160

Higgins J, Detweiler C. 2016. The waterbug sub-surface sampler: design, control and analysis. Daejeon, South Korea: IEEE Int Conf Int Robot Sys (IROS). p. 330–337. https://doi.org/10.1109/IROS.2016.7759075

Hoegh-Guldberg O, Cai R, Poloczanska ES, Brewer PG, Sundby S, Hilmi K, Fabry VJ, Jung S. 2014. The Ocean. *In:* Barros VR, Field CB, Dokken DJ, Mastrandrea MD, Mach KJ, Bilir TE, Chatterjee M, Ebi KL, Estrada YO, Genova RC, et al., editors. Climate change 2014: impacts, adaptation, and vulnerability. Part B: regional aspects. Contribution of working group II to the fifth assessment report of the Intergovernmental Panel on Climate Change. Cambridge and New York: Cambridge University Press. p. 1655–1731.

Honda MC, Watanabe S. 2007. Utility of an automatic water sampler to observe seasonal variability in nutrients and DIC in the Northwestern North Pacific. J Oceanogr. 63:349–362. https://doi.org/10.1007/s10872-007-0034-5

Jiang Z-P, Hydes DJ, Hartman SE, Hartman MC, Campbell JM, Johnson BD, Schofield B, Turk D, Wallace D, Burt WJ, et al. 2014. Application and assessment of a membrane-based pCO_2 sensor under field and laboratory conditions. Limnol Oceanogr Methods. 12(4):264–280. https://doi.org/10.4319/lom.2014.12.264

Kennedy EV, Perry CT, Halloran PR, Iglesias-Prieto R, Schonberg CH, Wisshak M, Form AU, Carricart-Ganivet JP, Fine M, Eakin CM, et al. 2013. Avoiding coral reef functional collapse requires local and global action. Curr Biol. 23(10):912–918. https://doi.org/10.1016/j.cub.2013.04.020

Lewis E, Wallace D. 1998. Program developed for CO_2 system calculations. ORNL/CDIAC-105. Carbon Dioxide Information Analysis Center, Oak Ridge National Laboratory. Oak Ridge, Tennessee: US Department of Energy. https://doi.org/10.3334/CDIAC/otg.CO2SYS_DOS_CDIAC105

Manzello DP, Enochs IC, Musielewicz S, Carlton R, Gledhill D. 2013. Tropical cyclones cause $CaCO_3$ undersaturation of coral reef seawater in a high-CO_2 world. J Geophys Res Oceans. 118(10):5312–5321. https://doi.org/10.1002/jgrc.20378

Martin JB, Thomas RG, Hartl KM. 2004. An inexpensive, automatic, submersible water sampler. Limnol Oceanogr Methods. 2(12):398–405. https://doi.org/10.4319/lom.2004.2.398

Martz TR, Connery JG, Johnson KS. 2010. Testing the Honeywell Durafet® for seawater pH applications. Limnol Oceanogr Methods. 8(5):172–184. https://doi.org/10.4319/lom.2010.8.172

Martz T, Daly K, Byrne R, Stillman J, Turk D. 2015. Technology for ocean acidification research: needs and availability. Oceanography (Washington DC). 28(2):40–47. https://doi.org/10.5670/oceanog.2015.30

Mehrbach C, Culberson CH, Hawley JE, Pytkowicz RM. 1973. Measurement of the apparent dissociation constants of carbonic acid in seawater at atmospheric pressure. Limnol Oceanogr. 18(6):897–907. https://doi.org/10.4319/lo.1973.18.6.0897

Moberg F, Folke C. 1999. Ecological goods and services of coral reef ecosystems. Ecol Econ. 29(2):215–233. https://doi.org/10.1016/S0921-8009(99)00009-9

Price NN, Martz TR, Brainard RE, Smith JE. 2012. Diel variability in seawater pH relates to calcification and benthic community structure on coral reefs. PLOS ONE. 7:e43843. https://doi.org/10.1371/journal.pone.0043843

Riebesell U, Fabry VJ, Hansson L, Gattuso JP. 2011. Guide to best practices for ocean acidification research and data reporting. Luxembourg: Publications Office of the European Union. Available from: https://doi.org/10.2777/66906

R Studio Team. 2015. RStudio: integrated development for R. Boston, Massachusetts: RStudio. Available from: http://www.rstudio.com/

Seidel MP, DeGrandpre MD, Dickson AG. 2008. A sensor for in situ indicator-based measurements of seawater pH. Mar Chem. 109(1–2):18–28. https://doi.org/10.1016/j.marchem.2007.11.013

Shaw EC, McNeil BI. 2014. Seasonal variability in carbonate chemistry and air–sea CO_2 fluxes in the southern Great Barrier Reef. Mar Chem. 158:49–58. https://doi.org/10.1016/j.marchem.2013.11.007

Shaw EC, McNeil BI, Tilbrook B. 2012. Impacts of ocean acidification in naturally variable coral reef flat ecosystems. J Geophys Res. 117:C03038. https://doi.org/10.1029/2011JC007655

Sutton AJ, Sabine CL, Maenner-Jones S, Lawrence-Slavas N, Meinig C, Feely RA, Mathis JT, Musielewicz S, Bott R, McLain PD, et al. 2014. A high-frequency atmospheric and seawater pCO_2 data set from 14 open-ocean sites using a moored autonomous system. Earth Syst Sci Data. 6:353–366. https://doi.org/10.5194/essd-6-353-2014

Wallace RB, Baumann H, Grear JS, Aller RC, Gobler CJ. 2014. Coastal ocean acidification: the other eutrophication problem. Estuar Coast Shelf Sci. 148:1–13. https://doi.org/10.1016/j.ecss.2014.05.027

Wickham H. 2009. ggplot2: elegant graphics for data analysis. New York: Springer-Verlag. Available from: https://ggplot2.tidyverse.org

Yoon TK, Jin H, Oh N-H, Park J-H. 2016. Technical note: assessing gas equilibration systems for continuous pCO_2 measurements in inland waters. Biogeosciences. 13:3915–3930. https://doi.org/10.5194/bg-13-3915-2016